Journal of Vacuum Science and Technology B

RESEARCH ARTICLE | AUGUST 19 2024

# Effects of athermal carrier injection on Co-60 gamma-ray damage in SiC merged-PiN Schottky diodes

**Special Collection:** Celebrating the Achievements and Life of Paul H. Holloway

Jian-Sian Li ; Chao-Ching Chiang ; Hsiao-Hsuan Wan ; Sergei P. Stepanoff ; Fan Ren ; Aman Haque ; Douglas Wolfe ; S. J. Pearton



*J. Vac. Sci. Technol. B* 42, 052203 (2024)
https://doi.org/10.1116/6.0003819

# Effects of athermal carrier injection on Co-60 gamma-ray damage in SiC merged-PiN Schottky diodes

Cite as: J. Vac. Sci. Technol. B **42**, 052203 (2024); doi: 10.1116/6.0003819
Submitted: 11 June 2024 · Accepted: 23 July 2024 ·
Published Online: 19 August 2024



Jian-Sian Li,[1,a)] Chao-Ching Chiang,[1] Hsiao-Hsuan Wan,[1] Sergei P. Stepanoff,[2,3] Fan Ren,[1] Aman Haque,[4] Douglas Wolfe,[2,3,5,6] and S. J. Pearton[7]

## AFFILIATIONS

[1]Department of Chemical Engineering, University of Florida, Gainesville, Florida 32611
[2]Materials Science and Engineering Department, The Pennsylvania State University, University Park, Pennsylvania 16802
[3]Applied Research Laboratory, The Pennsylvania State University, University Park, Pennsylvania 16802
[4]Department of Mechanical Engineering, The Pennsylvania State University, University Park, Pennsylvania 16802
[5]Engineering Science and Mechanics Department, The Pennsylvania State University, University Park, Pennsylvania 16802
[6]Ken and Mary Alice Lindquist Nuclear Engineering Department, The Pennsylvania State University, University Park, Pennsylvania 16802
[7]Department of Materials Science and Engineering, University of Florida, Gainesville, Florida 32611

**Note:** This paper is part of the Special Topic Collection Celebrating the Achievements and Life of Paul H. Holloway.
[a)]**Author to whom correspondence should be addressed:** jiansianli@ufl.edu



## ABSTRACT

Co-60 gamma irradiation of SiC merged-PiN Schottky (MPS) diodes up to fluences of 1 Mrad (Si) produces increases in both forward and reverse current, with less damage when the devices are biased during irradiation. Subsequent injection of minority carriers by forward biasing at 300 K can partially produce some damage recovery, but at high forward biases also can lead to further degradation of the devices, even in the absence of radiation damage. Recombination-enhanced annealing by carrier injection overall is not an effective technique for recovering gamma-induced damage in SiC MPS diodes, especially when compared to other near athermal methods like electron wind force annealing.



## I. INTRODUCTION

The radiation hardness of microelectronic and photonic devices is always of practical interest when these are used in extreme environments.[1,2] In the specific case of 4H-SiC transistors and radiation detectors, these have excellent stability against high gamma-ray exposures, with only small changes up to ~23 MGy.[3] The electrical and optical properties, such as carrier concentration, absorption bands, and defect luminescence, are all resistant to doses in the MGy range.[4–21] While displacement damage in SiC from ionizing particles such as protons are well-understood,[2,9] the effects of x rays and gamma rays is usually less clear-cut. To remove a C or a Si from their lattice position, energy greater than 21 and 35 eV is required.[2] In general, the carrier removal rates due to irradiation of SiC are more than an order of magnitude lower than for Si.[10–20,22] The performance of SiC detectors can deteriorate under high radiation doses, such as those exceeding 1 Mrad/s, primarily due to the presence of interface traps[21] and traps generated within dielectrics use for isolation and passivation.[23–30]

Gamma irradiations of up to 17 MGy [1700 Mrad (Si)] have been studied in SiC junction field-effect transistors (JFETs), resulting in positive threshold voltage shift up to 0.5 V and monotonic decrease in transconductance.[31] At total ionizing doses of 100 Mrad (Si), SiC JFETs manifest inherent resistance to ionizing radiation due to the absence of a gate insulator, typically displaying only marginal deviations in pinch-off voltage and transconductance.[30–32] Device designs incorporating substantial $SiO_2$ or other passivation layers tend to be more susceptible to gamma radiation.[19] SiC JFET devices for Venus exploration demonstrate ionizing radiation tolerance exceeding 7 Mrad (Si).[15,16]

The effects of γ-ray irradiation on 6H-SiC diodes have also been investigated extensively. Various research groups utilized a 60Co γ-ray source to expose the detectors to high doses. For doses of 120 kGy, a decrease in leakage current was observed, while at 1.080 MGy, the γ-ray detection efficiency of SiC photodiodes remained unchanged and at 2.5 MGy, a charge collection efficiency of 100% was measured in p-n SiC diodes.[18–21] Some recovery of the gamma-induced damage is observed after room temperature storage over periods of at least a week.[33]

While thermal annealing of defects in 4H-SiC requires high temperatures (often up to 800 °C), recombination-enhanced defect reactions are almost athermal in this material.[34–37] The theoretical framework for this type of carrier injection mechanism was elucidated by Weeks *et al.*[38]. The energy released during nonradiative electron or hole capture is primarily transformed into vibrational energy, which is initially confined to the area surrounding the defect. This localized vibrational energy can facilitate defect-related processes, such as diffusion.[38]

In this paper, we report an examination of forward-biased (hole) injection effects in gamma-irradiated SiC MPS diodes. There is only limited effectiveness of this approach for room temperature annealing of the gamma-induced degradation of the diodes.

## II. EXPERIMENT

The packaged 3.3 kV, 5A SiC merged-PiN Schottky (MPS) diodes were purchased from Gene SiC semiconductor. The diode forward current was 5A at ∼3 V forward bias. The packages were TO-363-7 model. The main applications for these devices are in switch mode power supplies, motor drives, and power factor correction systems. Merged-PiN Schottky (MPS) diodes effectively

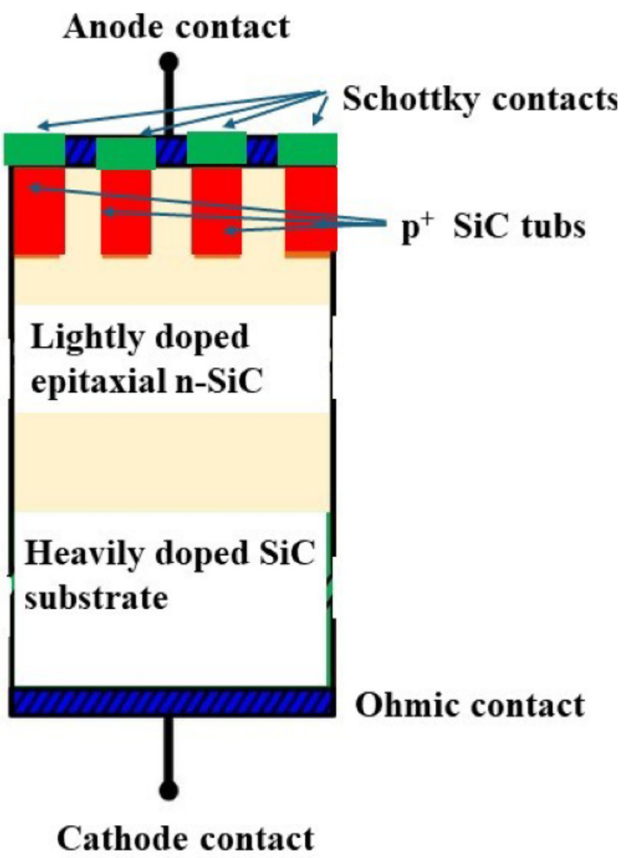


FIG. 1. Schematic of the SiC MPS diode.

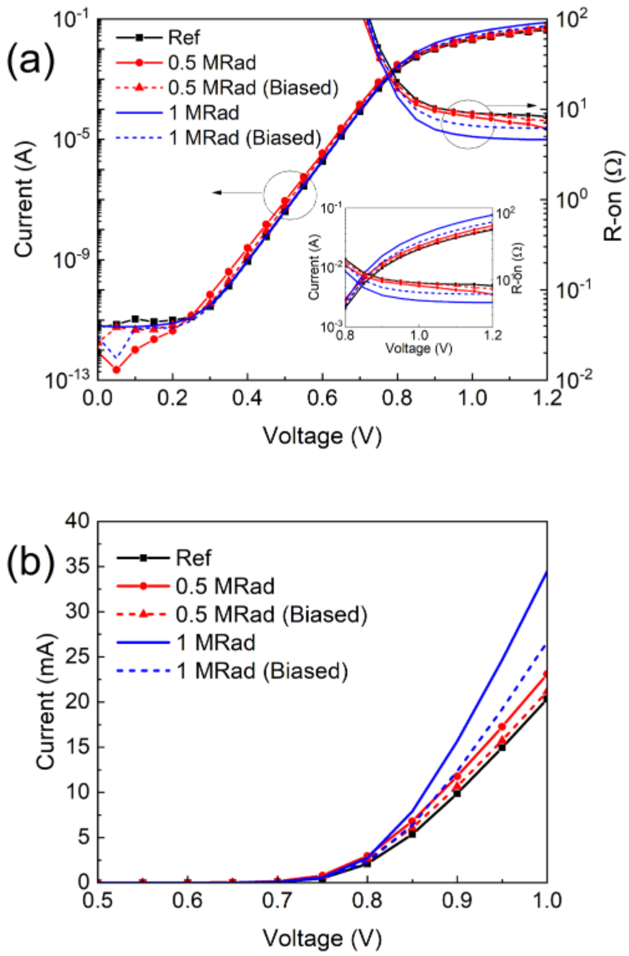


FIG. 2. (a) Forward I–V characteristics and $R_{ON}$ values from SiC MPS diodes as a function of Co-60 γ-ray fluence. (b) Expanded view of forward I–V characteristics from SiC MPS diodes as a function of Co-60 γ-ray fluence.

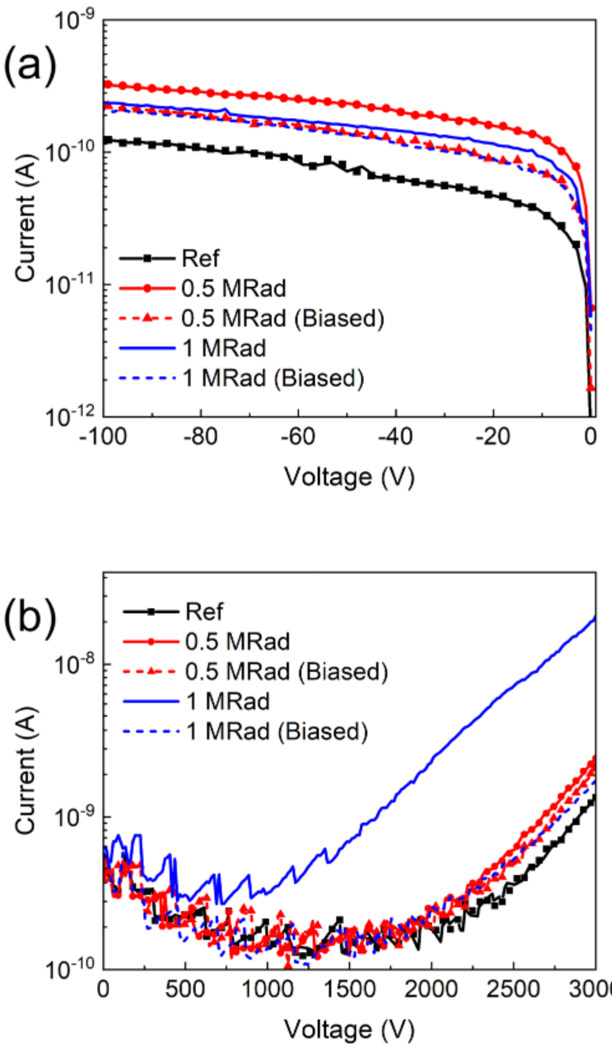


**FIG. 3.** (a) Reverse I–V characteristics from SiC MPS diodes at (a) low bias and (b) high bias and as a function of Co-60 γ-ray fluence.

combine Schottky diode and a P-N diode connected in parallel and are predicated upon the junction barrier Schottky (JBS) diode architecture, wherein $p^+$ regions are integrated into the active region. The p-n junctions engendered by these $p^+$ regions are activated under conditions of elevated current. This results in a substantial influx of minority carriers into the drift layer, thereby reducing resistivity and increasing current. Bipolar diodes utilize both electrons and holes as charge carriers to conduct current in their on-state and this results in conductivity modulation, where the presence of these carriers significantly reduces the resistance of the drift region during operation. While bipolar devices decrease on-state resistance, they have drawbacks, including increased power loss during switching between on and off states, and a higher potential barrier for current conduction. In contrast, unipolar diodes, like Schottky diodes, rely on a single type of charge carrier, either electrons or holes. As a result, their on-state resistance is typically higher for the same voltage rating compared to bipolar diodes. However, they offer faster switching speeds and lower potential barriers for current conduction. The merged-PiN Schottky (MPS) diode combines elements of both unipolar and bipolar devices, leveraging their respective advantages.

Consequently, MPS diodes have improved surge resilience relative to traditional JBS diodes, while also maintaining low forward voltage drop and reverse leakage current characteristics. Figure 1 shows a schematic of the MPS diode.

The current–voltage (I–V) characteristics were measured utilizing a Tektronix 370-A and a 371-B curve tracer, while an Agilent 4156C parameter analyzer facilitated forward and reverse current as well as capacitance–voltage (C–V) measurements. Samples

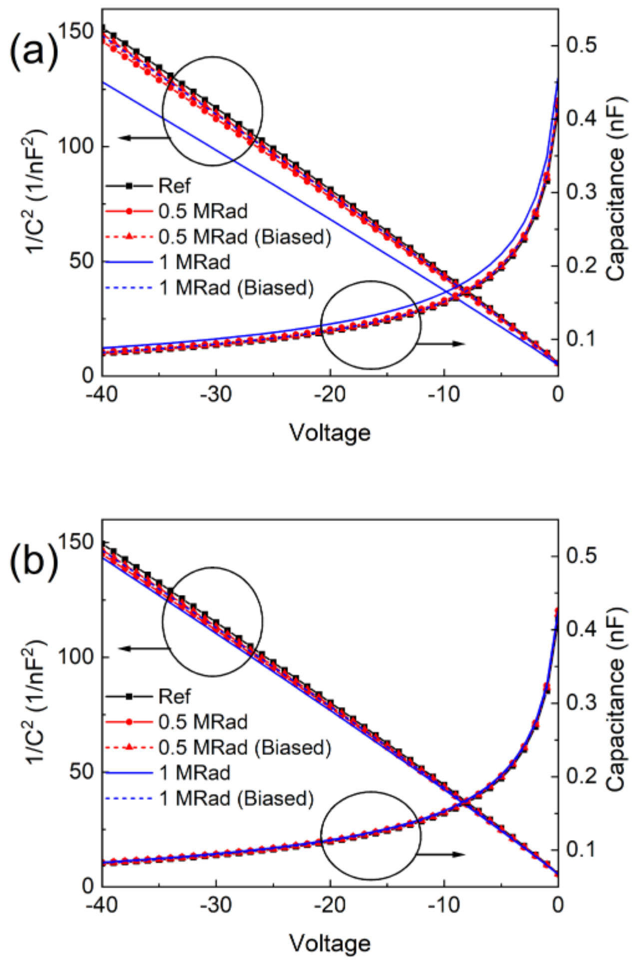


**FIG. 4.** C–V and $C^{-2}$–V characteristics to extract doping in the drift layer. (a) Before and after gamma irradiation. (b) Before and after forward bias in injection in unirradiated reference rectifiers.

**TABLE I.** Diode parameters as a function of gamma irradiation condition.

| As-irrad. | Current@1 V (mA) | $R_{ON}$@1 V (Ω) | $V_{ON}$ (V) | Current@-100 V (nA) | Current@-3 kV (nA) | Relative carrier conc. |
|---|---|---|---|---|---|---|
| Reference | 20.3 | 9.1 | 0.79 | 0.12 | 1.3 | 1 |
| 0.5 Mrad | 23.1 | 8.2 | 0.80 | 0.24 | 2.4 | 1.04 |
| 0.5 Mrad (biased) | 21.2 | 9 | 0.80 | 0.22 | 2.1 | 1.02 |
| 1 Mrad | 34.5 | 4.9 | 0.81 | 0.32 | 20.8 | 1.18 |
| 1 Mrad (biased) | 26.6 | 6.6 | 0.81 | 0.21 | 1.7 | 1.02 |

underwent irradiation with Co-60 γ-rays at the Penn State Radiation Science and Engineering Center within a 1 MW training, research, isotopes, and general atomics reactor core, utilizing a dry-lead shield gamma testing facility. The dose rate, certified by the National Institute of Standards and Technology, was approximately 180 krad/h (±∼10%), with samples irradiated to a fluence (Φ) of 1 Mrad, surpassing the generic requirement for radiation-hardened military electronics of 300 krad (Si) and meeting the "stretch" goal of 1 Mrad (Si). The irradiation setup comprised 60Co sources surrounding the samples, ensuring a relatively uniform dose

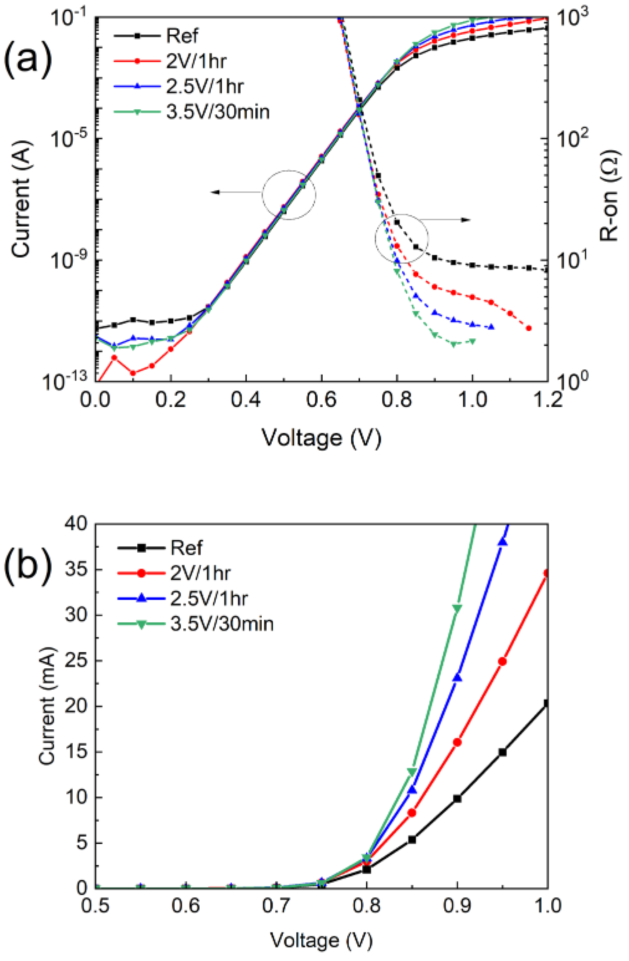


**FIG. 5.** (a). Forward I–V characteristics and $R_{ON}$ values from reference SiC MPS diodes. (b) Expanded view of forward I–V characteristics from reference SiC MPS diodes as a function of forward bias injection conditions.

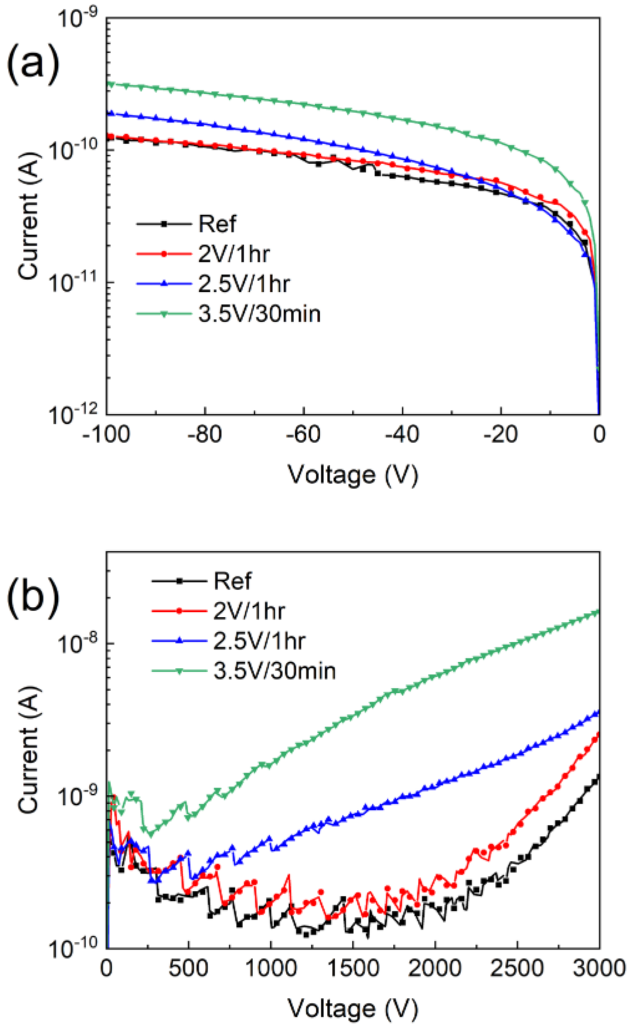


**FIG. 6.** (a) Reverse I–V characteristics and $R_{ON}$ values from reference SiC MPS diodes. (b) Expanded view of reverse I–V characteristics from reference SiC MPS diodes as a function of forward bias injection conditions.

**TABLE II.** Diode parameters as a function of postirradiation forward bias injection conditions.

| Forward annealing | Current @1 V (mA) | $R_{ON}$ @1 V (Ω) | $V_{ON}$ (V) | Current @-100 V (nA) | Current @-3 kV (nA) |
|---|---|---|---|---|---|
| Reference | 20.3 | 9.1 | 0.79 | 0.12 | 1.3 |
| 2 V, 1 h | 34.6 | 4.9 | 0.79 | 0.13 | 2.5 |
| 2.5 V, 1 h | 54.4 | 2.9 | 0.78 | 0.19 | 3.6 |
| 3.5 V, 30 min | 79.7 | 2.1 | 0.78 | 0.32 | 16.2 |
| 1 Mrad (as-irrad) | 34.4 | 5 | 0.81 | 0.24 | 20.8 |
| 2 V, 1 h | 36.6 | 4.7 | 0.81 | 0.21 | 11.4 |
| 2.5 V, 1 h | 37.4 | 4.6 | 0.81 | 0.17 | 6.9 |
| 3.5 V, 30 min | 58.1 | 2.7 | 0.80 | 0.29 | 24.6 |

rate within the irradiator, resulting in isotropic gamma dose distribution. The primary $^{60}$Co-60 gamma–photon lines were 1.17 and 1.33 MeV. Effective gamma-ray fluence was derived from the total ionizing dose using the conversion factor 1 rad (Si) = $2.0 \times 10^9$ photons/cm$^2$. The mean free path for the Co-60 gamma rays in SiC are ∼6 cm,[39] so they pass through the package and the entire SiC device structure. The total linear attenuation coefficient is ∼0.7 cm$^{-1}$ at these energies due to combined photoelectric absorption, coherent and incoherent scattering, and pair production. The MPS diodes were irradiated either with or without a reverse bias of −100 V.

## III. RESULTS AND DISCUSSION

Figures 2(a) and 2(b) show the forward I–V characteristics from the MPS rectifiers before and after gamma irradiation at the two different fluences and either irradiated with or without bias applied. The increase in current scales with fluence and is higher for unbiased devices, likely because the presence of a depletion region during irradiation can more effectively sweep charge from the sensitive volume. There was not any significant change in the ideality factor in the forward I–V, which would be most affected by interface trapping.

The same trends were observed in the reverse I–V characteristics of Fig. 3. Figure 3(a) shows the leakage at low biases, while Fig. 3(b) shows the current at high bias. Both show the same trends. Generation-recombination centers associated with deep-level traps created by the gamma-ray absorption processes within the bandgap are particularly effective at capturing and emitting carriers, significantly increasing the reverse leakage current. Since gamma rays mainly interact with the SiC through secondary processes, such as the production of secondary electrons (Compton scattering and photoelectric effect) and positrons (pair production), this leads to secondary electrons creating additional ionization and displacement damage as they travel through the rectifier. The reverse leakage current in a rectifier is strongly influenced by the concentration of generation-recombination centers because these centers facilitate the generation and recombination of charge carriers within the semiconductor. A higher concentration of these centers leads to more frequent generation of electron-hole pairs and, consequently, a higher reverse leakage current. The changes observed in forward and reverse current were not due to significant changes in the drift layer carrier concentration, as determined by the C–V characteristics of Fig. 4(a). The carrier density was slightly decreased at an effective carrier removal rate of <1 cm$^{-1}$. Table I summarizes the diode parameters as a function of irradiation condition.

We tried different forward bias injection condition on reference devices to determine the effects. Figures 5(a) and 5(b) show the forward current improved. Rasel *et al.* reported that use of current pulses can partially recover degradation due to forward bias stressing of 4H-SiC Schottky diodes.[40] In that work, the mechanism was identified as momentum transfer from the injected electrons to defects created by the electrical stressing, leading to motion and annealing of these defects. In our case, the recombination-enhanced annealing of defects is operative, as reported in previous work.[34–37] At too high a forward bias, the reverse current also increased, as

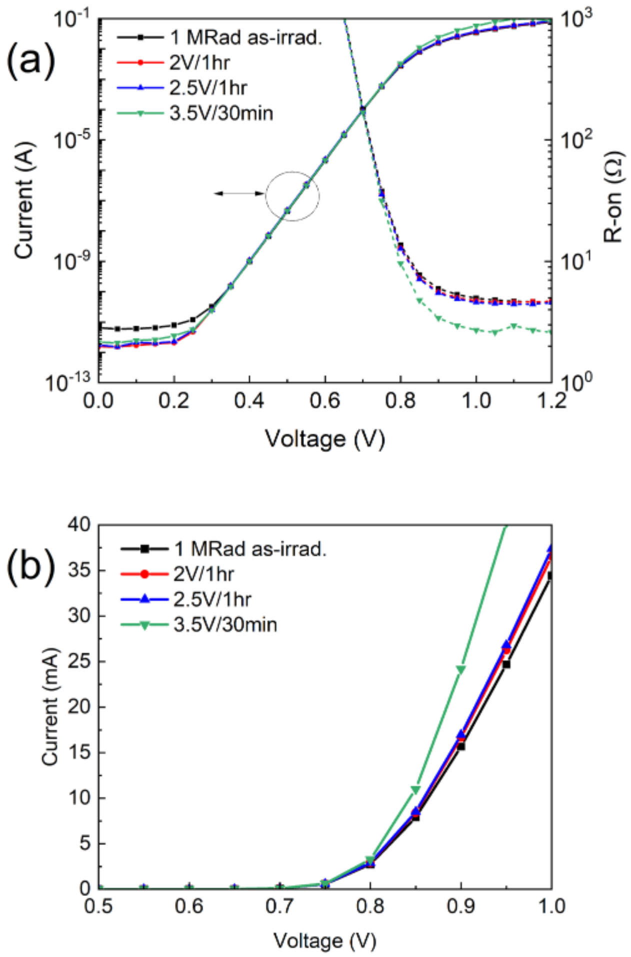


**FIG. 7.** (a) Forward I–V characteristics and $R_{ON}$ values from irradiated (1 Mrad, unbiased) SiC MPS diodes. (b) Expanded view of forward I–V characteristics from irradiated (1 Mrad, unbiased) SiC MPS diodes as a function of forward bias injection conditions.

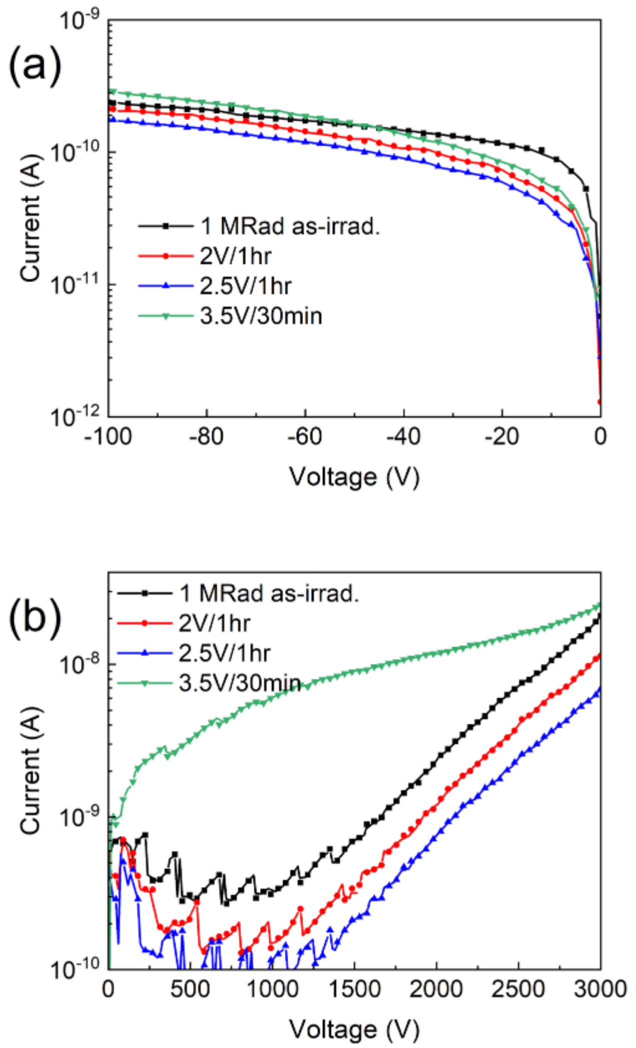


**FIG. 8.** (a) Reverse I–V characteristics and $R_{ON}$ values from irradiated (1 Mrad, unbiased) SiC MPS diodes. (b) Expanded view of reverse I–V characteristics from irradiated (1 Mrad, unbiased) SiC MPS diodes as a function of forward bias injection conditions.

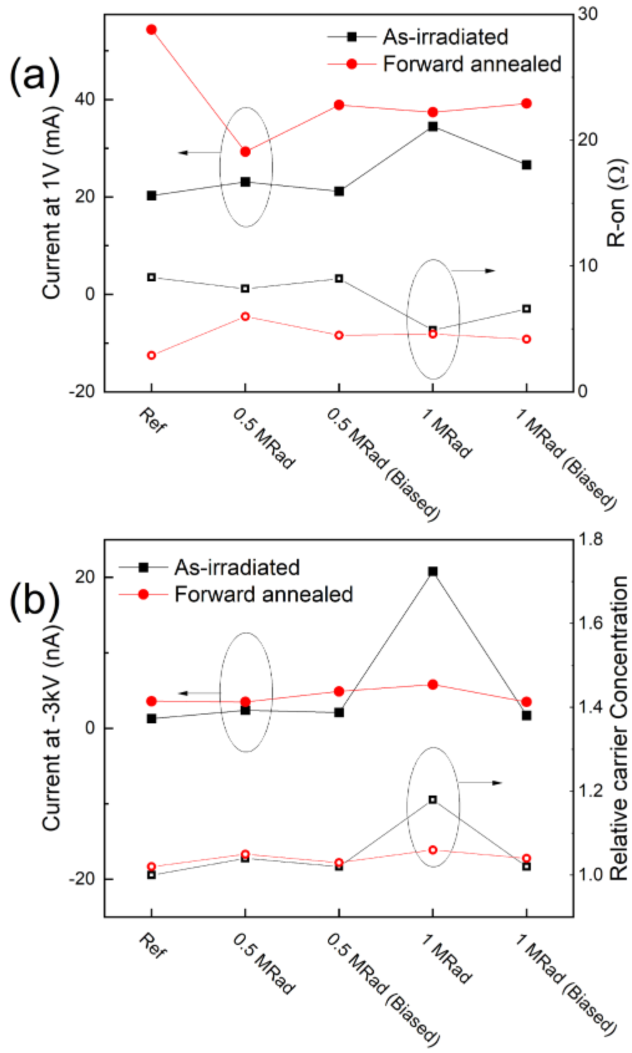


**FIG. 9.** (a) Forward current at 1 V bias and $R_{ON}$ values before and (b) reverse current at 3 kV bias and carrier density in the drift region after forward bias injection at 2.5 V.

shown in Figs. 6(a) and 6(b). This could be due to migration of dislocations or other extended defects into the drift regions.[35,36] It was not due to a change in carrier concentration in the drift regions, as evidenced by the fact that the C–V characteristics did not change [Fig. 4(b)]. Note that the magnitude of the reverse current at high biases is of the same order as devices subject to the highest gamma-ray fluence. In other words, use of an excessive forward bias injection condition degrades the device as much as the exposure to the gamma-ray irradiation. The minority carrier diffusion lengths in SiC are reported to be in the range 1–10 $\mu$m,[41,42] more than sufficient to produce recovery of the gamma-induced damage if recombination-induced defect annealing is present in the diodes. Table II summarizes the effect of different forward bias injection conditions on the diode parameters.

We chose the 2.5 V/1 h condition as the standard for examining its effect on damage recovery because it did not produce the degradation of the reference and 1 Mrad-irradiated diodes seen for the 3.5 V injection. However, even at this optimum condition, the 2.5 V/1 h forward annealing slightly degraded all the SiC diodes, except for the 1 Mrad (nonbiased) one, which showed significant recovery. Figures 7(a) and 7(b) show the forward I–V characteristics after carrier injection at 2.5 V, with little recovery to the reference values across the entire voltage range. Similar results were obtained for the reverse I–V characteristics, as shown in

**TABLE III.** Diode parameters as a function of postirradiation injection annealing at 2.5 V for 1 h.

| Forward annealing | Current@1 V (mA) | $R_{ON}$@1 V (Ω) | $V_{ON}$ (V) | Current@-100 V (nA) | Current@-3 kV (nA) | Relative carrier conc. |
|---|---|---|---|---|---|---|
| Reference | 20.3 | 9.1 | 0.79 | 0.12 | 1.3 | 1 |
| 0.5 Mrad | 29.3 | 6.0 | 0.82 | 0.19 | 3.5 | 1.05 |
| 0.5 Mrad (biased) | 38.9 | 4.5 | 0.81 | 0.28 | 4.9 | 1.03 |
| 1 Mrad | 37.4 | 4.6 | 0.81 | 0.17 | 5.8 | 1.06 |
| 1 Mrad (biased) | 39.2 | 4.2 | 0.81 | 0.34 | 3.5 | 1.04 |

Figs. 8(a) and 8(b). The reverse currents are still larger than in the unirradiated reference diodes. Certainly, the forward-biased carrier injection is much less effective than electron wind force annealing in improving the SiC diode characteristics. We want to emphasize that there is a region where there is some recovery of the damage after forward bias annealing, but if the forward bias is too large, the devices, including the reference diode, are degraded. This shows again the limitation of the carrier injection method for trying to repair radiation damage in SiC.

Figure 9(a) summarizes the change in forward current measured at 1 V for all the conditions examined, while Fig. 8(b) summarizes the reverse current values at 3 kV bias. The gamma-induced damage is only obvious at a fluence of 1 Mrad and biasing during radiation exposure reduces the increase in current. Forward bias injection always produces further degradation of the forward and reverse current, except in the case of the diode with the greatest amount of radiation damage (1 Mrad, unbiased). This shows the recombination-enhanced annealing mechanism is not generally applicable to gamma-damage in SiC MPS diodes and is not an effective technique for damage recovery at room temperature. Table III summarizes the effect of the forward bias injection at 2.5 V on the diode parameters.

## IV. SUMMARY AND CONCLUSIONS

The forward and reverse current of 4H-SiC MPS rectifiers increased after gamma-ray irradiation. The biasing of the diodes during the irradiation does help reduce the irradiation-induced degradation effect. Forward annealing at 2.5 V for 1 h was carried out to determine if minority carrier injection could produce recombination-enhanced point defect annealing at room temperature. After testing the reference and 1 Mrad-irradiated diodes up to 3.5 V, the diode dramatically degraded. The 2.5 V/1 h forward annealing condition slightly degraded all the SiC diodes, except for the 1 Mrad (nonbiased) one, which showed significant recovery. There is a small window of forward biasing conditions where there is some recovery of the damage after forward bias annealing, but at too large a forward bias, the MPS diodes are degraded, including the reference diode. This shows again the limitation of the carrier injection method for trying to repair radiation damage in SiC.

## ACKNOWLEDGMENTS

The work at UF was performed as part of Interaction of Ionizing Radiation with Matter University Research Alliance (IIRM-URA), sponsored by the Department of the Defense, Defense Threat Reduction Agency under Award No. HDTRA1-20-2-0002. The content of the information does not necessarily reflect the position or the policy of the federal government, and no official endorsement should be inferred.

## AUTHOR DECLARATIONS

### Conflict of Interest

The authors have no conflicts to disclose.

### Author Contributions

**Jian-Sian Li:** Methodology (equal); Writing – original draft (equal); Writing – review & editing (equal). **Chao-Ching Chiang:** Methodology (equal). **Hsiao-Hsuan Wan:** Methodology (equal). **Sergei P. Stepanoff:** Methodology (equal). **Fan Ren:** Conceptualization (equal); Methodology (equal); Writing – review & editing (equal). **Aman Haque:** Methodology (equal); Writing – review & editing (equal). **Douglas Wolfe:** Methodology (equal). **S. J. Pearton:** Conceptualization (equal); Methodology (equal); Writing – review & editing (equal).

## DATA AVAILABILITY

The data that support the findings of this study are available from the corresponding author upon reasonable request.

## REFERENCES

[1]D. A. Manyang Li, Chao Shen, Zhenyu Sun, Bo Xu, Chao Zhao, and Zhanguo Wang, Appl. Phys. Rev. **11**, 021315 (2024).
[2]F. Kyle Reed, K. C. Goetz, M. Nance Ericson, Daniel C. Sweeney, and N. Dianne Bull Ezell, "Wide bandgap semiconductors for extreme temperature and radiation environments," ORNL/TM-2021/2274, March 2022.
[3]F. H. Ruddy and J. G. Seidel, Nucl. Instrum. Methods Phys. Res. B **263**, 163 (2007).
[4]J. McGarrity, F. McLean, W. DeLancey, J. Palmour, C. Carter, J. Edmond, and R. Oakley, IEEE Trans. Nucl. Sci. **39**, 1974 (1992).
[5]M. De Napoli, Front. Phys. **10**, 898833 (2022).
[6]Takeshi Ohshima, Shinobu Onoda, Naoya Iwamoto, Takahiro Makino, Manabu Arai, and Yasunori Tanaka, "Radiation response of silicon carbide diodes and transistors," in *Physics and Technology of Silicon Carbide Devices*, edited by Y. Hijikata (IntechOpen, Rijeka, 2012).
[7]Indudhar Panduranga Vali, Pramoda Kumara Shetty, M. G. Mahesha, V. G. Sathe, D. M. Phase, and R. J. Choudhary, Nucl. Instrum. Methods Phys. Res. B **440**, 101 (2019).
[8]P. Vigneshwara Raja and N. V. L. Narasimha Murty, J. Appl. Phys. **123**, 161536 (2018).
[9]S. Onoda, T. Ohshima, T. Hirao, K. Mishima, S. Hishiki, N. Iwamoto, K. Kojima, and K. Kawano, IEEE Trans. Nucl. Sci. **54**, 1953 (2007).

[10]X. Liang, J. Cui, Q. Zheng, J. Zhao, X. Yu, J. Sun, D. Zhang, and Q. Guo, Radiat. Eff. Defects Solids **175**, 559 (2020).
[11]K. Murata *et al.*, Phys. Status Solidi A **214**, 1600446 (2017).
[12]J.-M. Lauenstein, M. C. Casey, R. L. Ladbury, H. S. Kim, A. M. Phan, and A. D. Topper, "Space radiation effects on SiC power device reliability," in *2021 IEEE International Reliability Physics Symposium (IRPS)* (IEEE, New York, 2021), pp. 1–8.
[13]J.-M. Lauenstein, P. G. Neudeck, K. L. Ryder, E. P. Wilcox, L. Chen, M. A. Carts, S. Y. Wrbanek, and J. D. Wraback, "Room temperature radiation testing of a 500 °C durable 4H-SiC JFET integrated circuit technology," in *2019 IEEE Radiation Effects Data Workshop* (IEEE, New York, 2019), pp. 1–7.
[14]B. Tala-Ighil, J.-L. Trolet, H. Gualous, P. Mary, and S. Lefebvre, Microelectron. Reliab. **55**, 1512 (2015).
[15]P. G. Neudeck, N. F. Prokop, L. C. Greer III, L. Y. Chen, and M. J. Krasowski, Mater. Sci. Forum **679–680**, 579 (2011).
[16]P. Neudeck, D. Spry, M. Krasowski, L. Chen, N. Prokop, L. Greer, and C. Chang, "Progressing −190 °C to +500 °C durable SiC JFET ICs from MSI to LSI," in *2020 IEEE International Electron Devices Meeting (IEDM)* (IEEE, New York, 2020), pp. 27–32.
[17]S. J. Pearton, Xinyi Xia, Fan Ren, Md Abu Jafar Rasel, Sergei Stepanoff, Nahid Al-Mamun, Aman Haque, and Douglas E. Wolfe, J. Vac. Sci. Technol. B **41**, 030802 (2023).
[18]H. Feng *et al.*, Electronics **12**, 2398 (2023).
[19]L. Shu, H. L. Liao, Z. Y. Wu, X. Y. Fang, S. W. Liang, T. D. Li, L. Wang, J. Wang, and Y. F. Zhao, Electronics **12**, 2194 (2023).
[20]P. Hazdra and S. Popelka, IET Power Electron. **12**, 3910 (2019).
[21]D. Hu, J. Zhang, Y. Jia, Y. Wu, L. Peng, and Y. Tang, IEEE Trans. Electron Devices **65**, 3719 (2018).
[22]V. V. Kozlovski, E. V. Bogdanova, V. V. Emtsev, K. V. Emtsev, A. A. Lebedev, and V. N. Lomasov, Mater. Sci. Forum **483–485**, 385 (2005).
[23]S. Krishnamurthy, R. Kannan, C. C. Kiong, T. B. Ibrahim, and Y. Abdullah, Int. J. Electr. Comput. Eng. Sci. **9**, 1453 (2019).
[24]A. Akturk, J. M. McGarrity, S. Potbhare, and N. Goldsman, IEEE Trans. Nucl. Sci. **59**, 3258 (2012).
[25]H. Feng *et al.*, J. Nanoelectron. Optoelectron. **16**, 1423 (2021).
[26]Indudhar Panduranga Vali, Pramoda Kumara Shetty, M. G. Mahesha, V. C. Petwal, Jishnu Dwivedi, D. M. Phase, and R. J. Choudhary, Vacuum **172**, 109068 (2020).
[27]F. Migliore *et al.*, Appl. Phys. Lett. **124**, 042101 (2024).
[28]F. Nava, E. Vittone, P. Vanni, G. Verzellesi, P. Fuochi, C. Lanzieri, and M. Glaser, Nucl. Instrum. Methods Phys. Res. A **505**, 645 (2003).
[29]S. Kang, J. Ha, J. Park, H. Kim, S. Chun, and Y. Kim, Nucl. Instrum. Methods Phys. Res. A **579**, 145 (2007).
[30]J. Park, S. Park, H. Shin, H. Kim, J. Kim, and S. Lee, J. Nucl. Sci. Technol. **51**, 482 (2014).
[31]Akinori Takeyama, Takahiro Makino, Yasunori Tanaka, Shin-Ichiro Kuroki, and Takeshi Ohshima, J. Appl. Phys. **131**, 244503 (2022).
[32]S. Metzger, H. Henschel, O. Kohn, and W. Lennartz, IEEE Trans. Nucl. Sci. **49**, 1351 (2002).
[33]Yun Li, Min Gong, Mingmin Huang, Yao Ma, and Zhimei Yang, Mater. Sci. Semicond. Process. **176**, 108331 (2024).
[34]L. Storasta, F. H. Carlsson, P. Bergman, and E. Janzén, Mater. Sci. Forum **483–485**, 369 (2005).
[35]E. E. Yakimov and E. B. Yakimov, J. Alloys Compd. **837**, 155470 (2020).
[36]M. Skowronski, J. Q. Liu, W. M. Vetter, M. Dudley, C. Hallin, and H. Lendenmann, J. Appl. Phys. **92**, 4699 (2002).
[37]Bin Chen, Hirofumi Matsuhata, Takashi Sekiguchi, Takasumi Ohyanagi, Akimasa Kinoshita, and Hajime Okumura, Appl. Phys. Lett. **96**, 212110 (2010).
[38]John D. Weeks, J. C. Tully, and L. C. Kimerling, Phys. Rev. B **12**, 3286 (1975).
[39]F. C. Hila *et al.*, Radiat. Phys. Chem. **182**, 109331 (2021).
[40]Md Abu Jafar Rasel, Nahid Sultan Al-Mamun, Sergei Stepanoff, Aman Haque, Douglas E. Wolfe, Fan Ren, and Stephen J. Pearton, Appl. Phys. Lett. **122**, 204101 (2023).
[41]T. Hatayama, H. Yano, Y. Uraoka, and T. Fuyuki, Microelectron. Eng. **83**, 30 (2006).
[42]Alexander Y. Polyakov, Qiang Li, Sung Wook Huh, Marek Skowronski, Olena Lopatiuk, Leonid Chernyak, and Edward Sanchez, J. Appl. Phys. **97**, 053703 (2005).